Performance Assessment of Biomass-derived Urea-Furfuraldehyde Resins as Oilfield Scale Inhibitors

Victor-Oji, C. O. [a,b*], Una, D.[a,c], and Akaranta, O.[a,b]

[a] *World Bank Africa Centre of Excellence for Oilfield Chemicals Research, University of Port Harcourt Nigeria.*
[b] *Department of Pure and Industrial Chemistry, University of Port Harcourt, Nigeria.*
[c] *Department of Petroleum and Gas Engineering, University of Port Harcourt, Nigeria.*

Authors' contributions

This work was carried out in collaboration among all authors. Author VOCO prepared the manuscript, synthesized the chemical derivatives, and interpreted the spectral data. Author UD conducted the experiments and did formal analysis. Author AO conceptualized, designed and supervised the study. All authors read and approved the final manuscript.

Original Research Article

ABSTRACT

Oilfield-scale formation is a persistent challenge in the oil industry. While numerous scale inhibitors have been in use for decades, there is a significant research gap in discovering renewable, cost-effective, ecologically friendly, and efficient inhibitors. This study sets out to fill this gap by investigating the potential of scale inhibitors (SIs) made from bio-resin derivatives of red onion skin; ROF and ROFU, in reducing $CaCO_3$ and $CaSO_4$ scales. The scale inhibition performance of ROF and ROFU was rigorously evaluated using the NACE standard static bottle test method. The data revealed that increasing scale-inhibitor contact time, concentration, and temperature enhances

_____

*Corresponding author: E-mail: cynthia.anyanwu@uniport.edu.ng;

inhibitor efficacy, with the best inhibition efficiencies found for ROF and ROFU on the $CaSO_4$ scale compared to the $CaCO_3$ scale across all studied parameters. A comparison of the prepared SIs with a commercial scale inhibitor (CSI) showed a high inhibition rate of over 90% at minimal dosage of 60ppm in both scales studied. Despite having a lower inhibition rate (IE) than CSI, ROF and ROFU demonstrate significant potential as green oilfield SIs. This sustainable technique, which transforms agro-waste into a valuable oilfield chemical via a one-pot chemical process, could have profound economic and societal benefits, offering hope for a more sustainable future in the oil industry.

1. INTRODUCTION

A sustainable future may see a large contribution from biomass, an adaptable and renewable resource. Agricultural food wastes and by-products with significant bioactive chemicals are produced in large quantities worldwide, particularly along the whole supply chain. Evaluating food waste as valuable biomass that may be turned into profitable products rather than an unmanageable waste stream has begun [1,2]. Food waste can produce biofuels, enzymes, antioxidant extracts, new biodegradable materials, electricity, and other commercial items because it is cheap and renewable [3].

Biobased chemicals are drawing more attention as sustainable substitutes in several industries, including oil and gas [4]. Within the petroleum sector, oilfield scale deposition is a frequent difficulty that results in lower production efficiency and higher operating expenses. Scale formation happens when precipitated minerals, like calcium carbonate ($CaCO_3$), calcium sulphate ($CaSO_4$) and/or barium sulfate ($BaSO_4$), settle on wellbore surfaces, pipelines, and downhole equipment from generated water. These deposits can harm equipment, drastically lower flow rates, and plug holes, resulting in expensive interventions. Scale development is a major concern in oilfield operations, impacting equipment integrity and production efficiency. Traditional scale inhibitors are often made from petroleum-based compounds, despite rising interest in sustainable alternatives, however, the limited availability and environmental impact of chemicals derived from fossil fuels have spurred the investigation of biobased substitutes [5-8].

Green oilfield scale inhibitors made of biobased materials provide several environmental and sustainability advantages. The carbon footprint associated with oilfield activities can be greatly decreased by substituting renewable chemicals for petroleum-based ones. Additionally, biobased inhibitors provide a more sustainable method of producing oil and gas and help protect nonrenewable resources [9,10]. These environmentally friendly substances may also be biodegradable, lessening their negative effects on aquatic environments and ecosystems. In conclusion, a viable path toward environmentally responsible and sustainable operations in the oil and gas sector is using biobased compounds as green oilfield scale inhibitors as these substitutes have the ability to lessen scale deposition while also lessening the environmental effect of conventional petroleum-based inhibitors by utilizing renewable resources [11].

Red onion skin (ROS) is one of the renewable feedstocks that has been used to create biomass-derived resins, such as ROSE-glutaraldehyde (ROG), ROSE-furfuraldehyde (ROF), and ROSE-urea furfuraldehyde (ROFU) resins [10-16]. In ROFU resins, furfuraldehyde and urea react via a one-pot, two-step process to generate a crosslinked polymer structure, which has the potential to mitigate scale formation due to their distinct chemical makeup. Their regenerative nature and possible scale inhibition features make them an attractive alternative (Husna et al., 2022). By comparing ROFU resins to their conventional counterpart using the National Association of Corrosion Engineers (NACE) standard bottle tests under simulated oilfield conditions, this work explores the possibilities of bio-based resins generated from urea-furfuraldehyde as oilfield scale inhibitors, considering their synthesis, characterization, and effectiveness in preventing scale formation in terms of its inhibition efficiency, compatibility and thermal stability in other chemicals, and likely environmental impact.

The utilization of bio-based derived resins of this kind, which have not been thoroughly investigated for this purpose, makes this study innovative, and the findings of this study will

advance sustainable solutions in petroleum and gas production and contribute to creating scale inhibitors for the oil and gas sector that are biodegradable and more environmentally friendly substitutes for currently used inhibitors by lowering their environmental impact and increasing production efficiency.

2. MATERIALS AND METHODS

2.1 Materials

Red onion skin (ROS) was sourced locally from the Oil Mill Market (4.8585°N, 7.0648°E) in Obio-Akpor Local Government Area, Rivers State, Nigeria. The analytical grade chemicals purchased from local suppliers include Urea, Furfuraldehyde, Sodium Hydroxide, Acetone, Sodium chloride, Calcium chloride dihydrate, Magnesium chloride hexahydrate, Sodium sulphate, sodium hydrogen carbonate, and Sodium carbonate. They were used as received without further purification.

2.2 Methods

The methodology employed during this study includes extraction of the biomass (Red onion Skin, ROS), chemical modification of ROS extract (ROSE), characterization of the chemically modified extracts, formulation and characterization of synthetic brine, formulation of the scale inhibitor (SI) solutions, and comparative assessment of the formulated scale inhibitor with a commercial scale inhibitor via static bottle test.

2.2.1 Extraction of ROS

The inedible outer skin of the red onion was thoroughly selected, cleaned, and sun-dried for about 6 hours. The dried red onion skin (ROS) was milled, sieved to 150μm particle size, and extracted by solvent extraction using acetone as described by Una et al. [17]. The ROS extract, ROSE, was concentrated using a rotary evaporator and dried in an oven at 55 ℃. The dried extract was stored in an airtight container labeled ROSE for further use.

2.2.2 Formulation of Synthetic brine

Synthetic brine was simulated in the laboratory to replicate formation brine by dissolving specific inorganic salts in distilled water according to the National Association of Corrosion Engineers (NACE) standard method, TM0197-2010. Synthetic brine was prepared by mixing solutions A and B, defined as calcium-containing brine and carbonate or sulfate-containing brine for $CaCO_3$ and $CaSO_4$ scale types, as outlined in Table 1, with distilled water in a 1:1 ratio. The formulated brines for $CaCO_3$ and $CaSO_4$ were filtered through a 0.45 μm membrane filter paper to remove undissolved salts.

2.2.3 Synthetic brine characterization

The physicochemical properties of synthetic brine, such as pH, density, salinity, conductivity, turbidity, dissolved oxygen, and alkalinity, were electrometrically analyzed for each studied scale type using the Horiba water monitor (U-52 model).

2.2.4 Chemical modification of ROSE

The biomass extract, ROSE, was modified via a one-pot condensation reaction with varying mixing ratios of ROSE: Furfural and ROSE: Furfural: Urea in an alkaline catalyst to give ROF and ROFU, respectively. For ROF, a reaction mixture of ROSE: Furfuraldehyde (2:1 mole ratio) was charged into a pre-weighed reactor vessel gradually heated to 120°C with continuous stirring under reflux for 60 min in the presence of a catalytic quantity of NaOH (based on ROSE), while for ROFU, a reaction mixture of furfuraldehyde: urea (2:1 mole ratio) was charged into a pre-weighed reactor vessel and refluxed continuously at a temperature of 70°C for 30 mins after which 2 moles of ROSE and a catalytic amount of NaOH was introduced into the mixture. This mixture was refluxed for 60 min with continuous stirring at 70°C; at the end of the reaction (when the volume of water condensed in the dean and stark trap is constant), the products

**Table 1. Composition of Synthetic water and test condition**

Scale Type	Brine Concentration, g/L
$CaSO_4$ (A+B)	A. **Calcium Containing Brine:** NaCl = 7.50, $CaCl_2.2H_2O$ = 11.10
	B. **Sulphate Containing Brine**: NaCl = 7.50, Na_2SO_4 = 10.66
$CaCO_3$ (A+B)	A. **Calcium Containing Brine:** $CaCl_2.2H_2O$ = 12.15, $MgCl_2.6H_2O$ = 3.68
	B. **Carbonate Containing Brine**: $NaHCO_3$ = 7.36, $NaCO_3$ = 33.0

were cooled, weighed, and stored in airtight containers labeled ROSE-furfuraldehyde (ROF) and ROSE-Furfuraldehyde-Urea (ROFU) resin respectively for later use. The proposed synthetic routes for ROF and ROFU are depicted in Schemes 1 and 2.
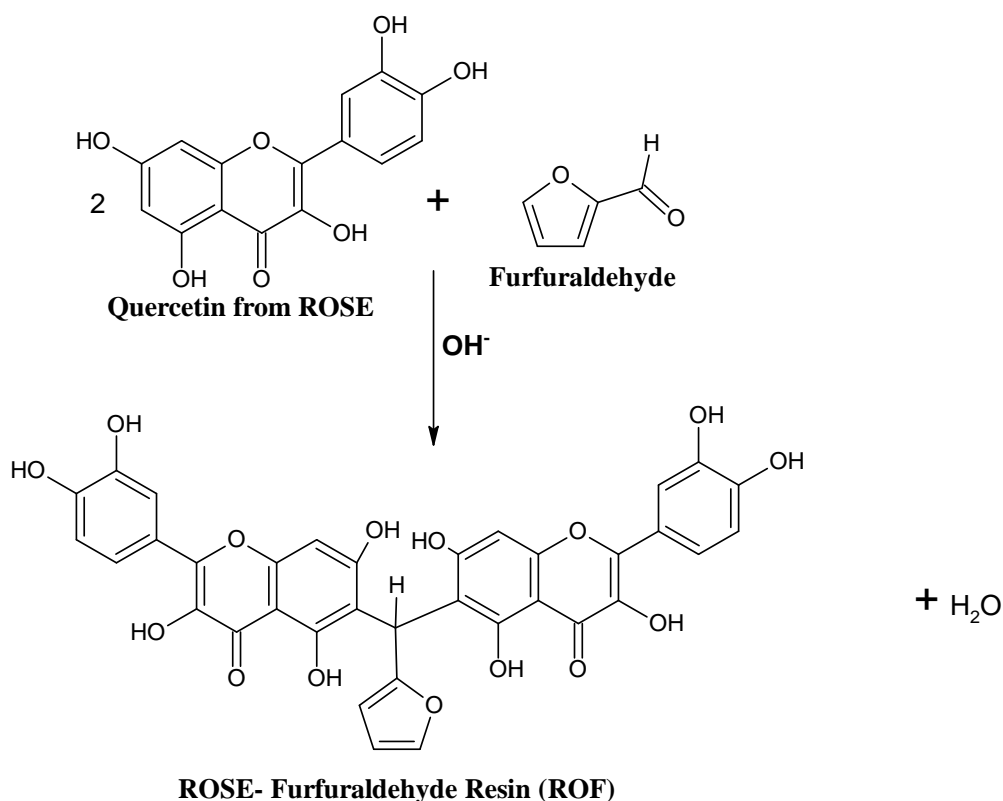
Scheme 1. Proposed reaction of ROSE with Furfuraldehyde in 2:1 molar ratio
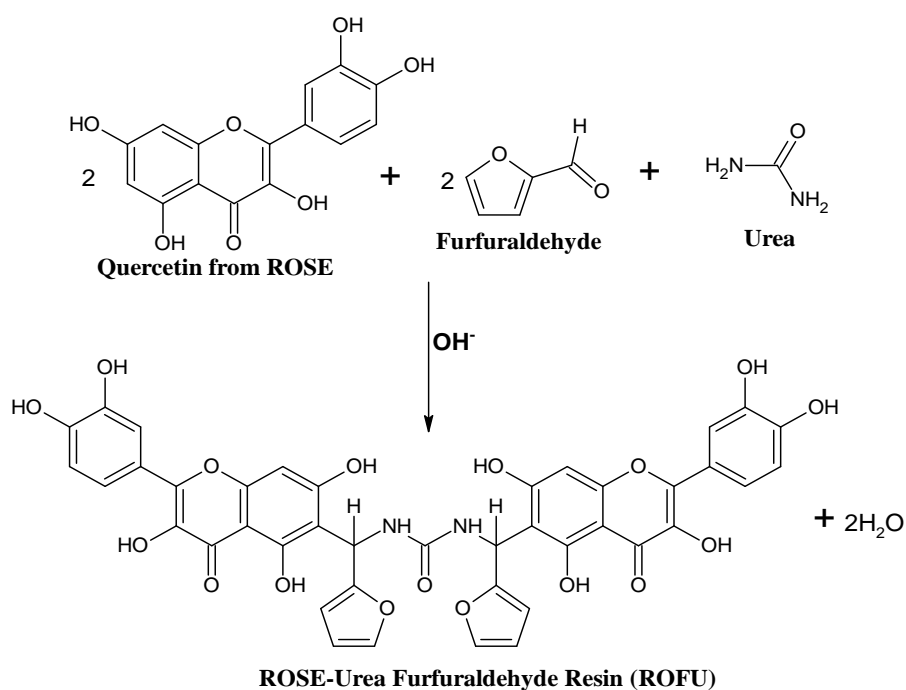
Scheme 2. Proposed reaction of ROSE with Furfuraldehyde and Urea in 2:2:1 molar ratio

2.2.5 Characterization of ROF and ROFU

ROSE, ROF, and ROFU were characterized using an Agilent Fourier-transform infrared (FTIR) spectrophotometer scanning in the 4000 – 650cm^{-1} range to detect the presence of functional groups. The pH, color, appearance, and solubility of ROSE, ROF, and ROFU in water were also determined. Scanning Electron Microscopy (SEM) was used to determine the morphology of the scale crystals formed before and after precipitation. This characterization was done for the calcium sulfate and carbonate-containing brines in the presence and absence of the formulated scale inhibitors ROF and ROFU.

2.2.6 Scale inhibitor evaluation tests

The modified ROSE derivatives, ROF and ROFU, were evaluated to ascertain their competency to function as scale inhibitors. The assay, which includes pH, thermal stability, and compatibility tests, determines whether they meet the set criteria for scale inhibitors before performance evaluation via the static bottle test method. The procedure for each test is outlined below, and the pass or fail criterion for each test is given in Table 2.

pH tests: The pH values were measured using an ORP pH meter calibrated with two buffer solutions of pH = 4.0 and 10.0.

Thermal Stability tests: Fifteen milliliters of each test inhibitor were introduced into Erlenmeyer flasks and examined for clarity. They were then transferred to a high-pressure, high-temperature (HPHT) vessel and heated to 130°C for 24 hours. After that, the vessel was taken out of the oven and placed in a desiccator to cool for two hours. The formulated inhibitors were thereafter transferred to a clear bottle and examined for changes in appearance because of the high-temperature impact on the solutions.

Brine compatibility tests: The brine compatibility with the formulated scale inhibitors and SIs was evaluated at 25°C and 90°C. Before the compatibility test, the synthetic brine was filtered using a 45 μ filter paper into a transparent 15 mL glass tube. The formulated SIs were then mixed with brine to cover the range of concentration studied (20 ppm - 100 ppm). The glass tubes were checked for signs of incompatibility, such as cloudiness/haziness and precipitation.

2.2.7 Scale inhibitor performance evaluation test

Standard test methods were used to evaluate the scale inhibition potential of the formulated scale inhibitors to mitigate the precipitation of oilfield scales under laboratory conditions. This study utilizes the National Association of Corrosion Engineers (NACE) standard static bottle test method, NACE TM0374-2007, to assess the inhibitor's ability to mitigate precipitation of calcium sulfate and calcium carbonate scales from solution at various scale inhibitor concentrations under static laboratory conditions as well as their thermal stability under the conditions listed in Table 3. The static bottle test involves incubating scaling brines mixed in 100 ml Erlenmeyer bottles for a stipulated period before being dosed with the formulated inhibitors, as shown in Fig. 1.

Fig. 1. Static bottle testing

Table 2. Inhibitor evaluation criterion

TEST	PASS	FAIL
pH for 100% product	> 5	< 5
Thermal stability at 130 ℃	Clear with or without a change in the color	Precipitation
Compatibility with water	Clear solution for all ranges of concentration (20ppm - 100 ppm) at both 25 ℃ and 90 ℃	Slightly Hazy, Hazy, or precipitated solution

Table 3. List of evaluated products and evaluation parameters

Product	ID	Evaluated Scale types	Evaluation conditions
ROSE-Furfuraldehyde resin	ROF	CaCO₃ and	71 °C & 90 °C, 22 hrs
ROSE-Urea -Furfuraldehyde resin	ROFU	CaSO₄ scales	71 °C, 4 hrs
Commercial scale inhibitor	CSI		

The precipitation of $CaCO_3$ and $CaSO_4$ salts from the brine, if any, is followed by a measurement of the concentration of calcium ions as a function of time as described in American Society for Testing and Materials (ASTM) test methods D511. The average Ca^{2+} values in mg/L of $CaSO_4$ or $CaCO_3$ retained in solution for the blank and each studied test concentration is defined as the percentage inhibition efficiency (IE) of the inhibitor and calculated using Equation 1:

$$\% \text{ Inhibition} = \frac{C_a - C_b}{C_c - C_b} \times 100 \qquad (1)$$

Where: C_a = Ca^{2+} concentration in the treated sample after precipitation

C_b = Ca^{2+} concentration in the blank after precipitation

C_c = Ca^{2+} concentration in the blank before precipitation

3. RESULTS AND DISCUSSION

3.1 Synthetic Brine Characterization

The physicochemical analysis of laboratory-simulated produced water and seawater was done, and the results are presented in Table 4.

Table 4. Physico-chemical assay of the synthetic brine

Parameter	Scale Type	
	CaSO₄	CaCO₃
pH	8.27	7.69
Density (g/cm³)	1.026	1.036
Temp ºC	25.3	25.1
Salinity	11.6	29.8
Turbidity (NTU)	171	185
Conductivity (ms/cm)	19.5	45.8
DO (mg/l)	7.72	7.76
Total Alkalinity (mg/l)	19	0.6

3.2 Characterization of ROF and ROFU

The pH, color, appearance, and solubility of ROSE, ROF, and ROFU in water have been assessed. The results show they are very soluble in water, dark brown in color, and have pH values of 8.0, 7.5, and 7.5, respectively, higher than the norm for scale inhibitors (pH > 5) (Table 2). Hence, they are ideal for use as oilfield scale inhibitors.

The bio-derived resins were subjected to FTIR spectroscopic analysis to confirm the presence of appropriate functional groups. The FTIR spectra of furfuraldehyde, urea, ROSE, and the resins, ROSE-furfuraldehyde resin (ROF) and ROSE-furfuraldehyde-urea resin (ROFU), are shown in Figs. 2 and 3, respectively. For ROF, a broad absorption peak due to phenolic O–H stretch vibration was observed at 3272 cm⁻¹, followed by strong doublet absorption peaks at 2851 cm⁻¹ and 2918 cm⁻¹ due to aromatic C–H and C=O stretch vibrations, which are characteristic of quercetin structure. A mix of aryl conjugated C=C and C=O stretch vibrations were observed at 1622 cm⁻¹ and 1562 cm⁻¹ alongside medium absorption bands at 1462 cm⁻¹ and 1443 cm⁻¹, which match aromatic C=C and =C–H stretch vibrations, the bands observed at 1380 cm⁻¹ and 1339 cm⁻¹ correspond to a combination of aryl O–H deformation and C–O stretch vibrations. Aromatic =C–H in-plane deformation vibration and out-of-plane C–H deformation within the furan ring were observed at 1272 cm⁻¹ and 1175 cm⁻¹, respectively, confirming the bond formation between ROSE and furfuraldehyde. The weak absorption band at 1052 cm⁻¹ is due to ether C–O stretch vibration, while that at 1019 cm⁻¹ corresponds to the furan ring's =C–H stretch vibrations. Strong to weak absorption bands seen at 888 cm⁻¹ and 784 cm⁻¹ correspond to aromatic and out-of-plane C–H stretching and deformation (due to isolated H atoms) vibrations, respectively, while the band at 724 cm⁻¹ is due to O–H out-of-plane bending vibrations. It is important to note that the disappearance of the characteristic C=O stretch vibrations of the aldehydic group in furfuraldehyde at 1782 cm⁻¹ and 1670 cm⁻¹ further affirms bond formation between ROSE and furfuraldehyde [14].

For ROFU, the overlying broad absorption peaks at 3350 cm⁻¹, 3290 cm⁻¹, and 3134 cm⁻¹ coincide with N–H and phenolic O–H stretch vibrations in the ROSE-furfuraldehyde-urea resin structure

(Scheme 2). The quercetin-characteristic doublet absorption peaks observed at 2851 cm⁻¹ and 2918 cm⁻¹ conform to aromatic C–H and C=O stretch vibrations, respectively. A mix of aryl conjugated –C=C and –C=O stretch vibrations was observed at 1622 cm⁻¹ and 1562 cm⁻¹; however, the band at 1592 cm⁻¹ corresponds to N–H deformation and C–N stretch vibration, while the appearance of a sharp peak at 1465 cm⁻¹ corresponds to the asymmetric N–CO–N stretch vibration, confirming the occurrence of an amide bond within the ROFU resin structure.

Stretch vibrations of aromatic C=C and =C–H in the furan ring were observed at 1443 cm⁻¹, while aryl O–H deformation and C–O stretch vibrations for the flavone ring occurred at 1387 cm⁻¹. Medium doublet peaks at 1357 cm⁻¹ and 1328 cm⁻¹ occur due to C–N stretch vibrations, while aromatic =C–H in-plane deformation vibration was observed at 1279 cm⁻¹. Weak absorption bands due to ether C–O stretch vibrations in the furan and flavone rings were also observed at 1264 cm⁻¹, 1223 cm⁻¹, 1197 cm⁻¹, 1179 cm⁻¹, 1127 cm⁻¹, and 1096 cm⁻¹, respectively.

Vibrations due to methine C–H deformation and aromatic =C–H stretch in the furan and flavone rings were observed at 1071 cm⁻¹ and 1015 cm⁻¹, respectively. The absorption peaks at 933 cm⁻¹ and 888 cm⁻¹ conform to out-of-plane aromatic C–H deformation vibrations (due to isolated H atoms) around the rings, while that at 817 cm⁻¹ corresponds to ether C–O–C stretching vibrations [14].

3.3 Scale Inhibitor Evaluation

The thermal stability and compatibility of the formulated scale inhibitors (SIs); ROF and ROFU, in the synthetic brine, were evaluated under laboratory conditions. They were found to be thermally stable after thermal exposure to temperatures up to 130°C, as no precipitation was observed, thus passing the criterion as depicted in Table 2. The compatibility tests with the synthetic brine were conducted at 25 °C and 90 °C for 24 hours and 15 minutes, respectively. No precipitation was observed for the studied period and specific temperatures, as the inhibitor solutions were clear, which signifies brine compatibility.
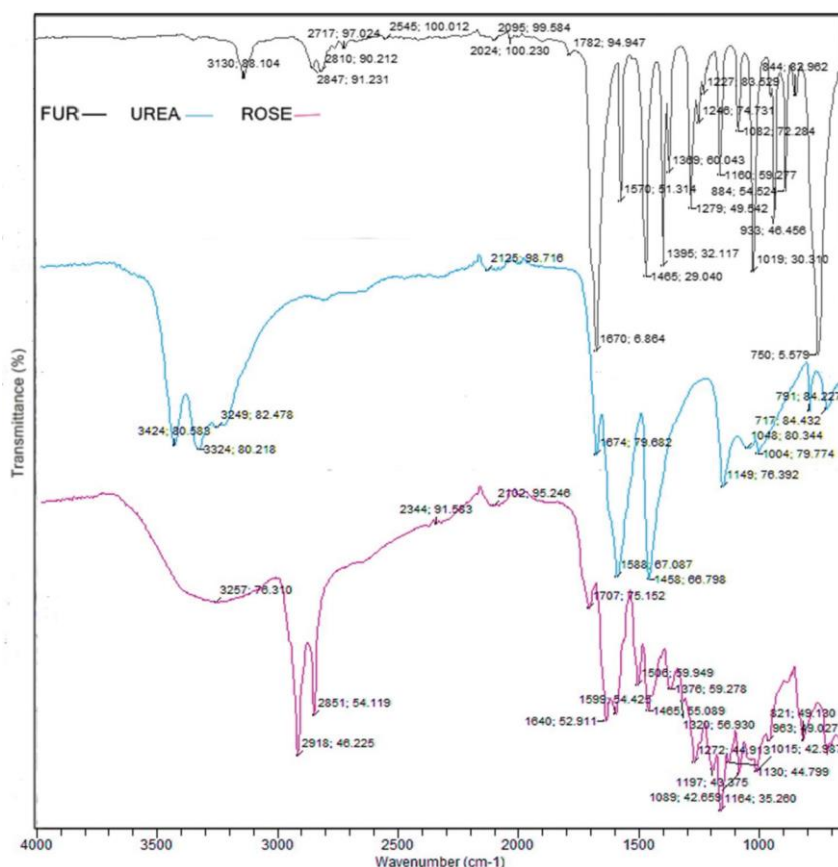

Fig. 2. FTIR Spectra of Furfuraldehyde (FUR), Urea, and Red Onion Skin Extract (ROSE)
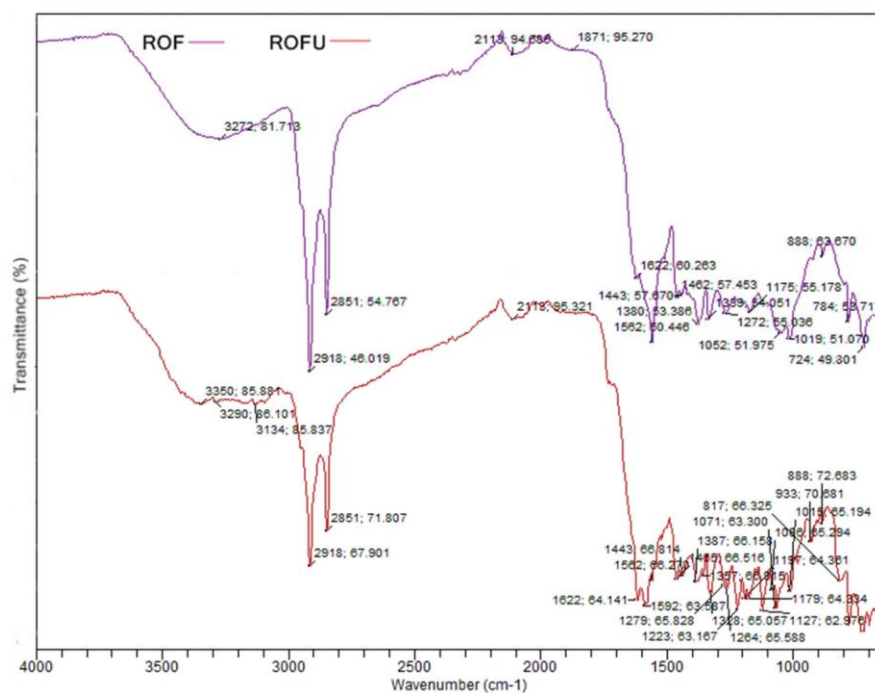
Fig. 3. FTIR spectra of ROSE-furfuraldehyde resin (ROF) and ROSE-formaldehyde-urea resin (ROFU)

3.4 SEM Micrographs of Scale Inhibition with ROF and ROFU

When a scale inhibitor is introduced to a sample brine, the size and shape of the scale crystal can indicate the degree of inhibitor dispersion. As posited by Mavredaki et al. [18], the higher the degree of crystal distortion, the smaller the crystal size, the greater the dispersibility, and the better the scale inhibition performance.

The SEM micrographs of $CaSO_4$ and $CaCO_3$ scales before and after conditioning in the absence and presence of low dosage of the prepared inhibitors, ROF and ROFU, are illustrated in Figs. 4 and 5. The loose-scale crystals in the incubated blank (Figs. 4a and b) became denser with well-defined crystal morphology on the addition of ROF to the $CaSO_4$ brine (Fig. 4c). However, with the addition of ROFU, the scale crystals are decreased in size and density and are well dispersed (Fig. 4d). They are also rhomboid-like, which indicates scale crystal growth inhibition [11,19].

Unlike the $CaSO_4$ brine, the scale crystals in the $CaCO_3$ brine are loosely but densely packed before incubation (Fig. 5a); however, after incubation, they become dense clusters with a defined shape (Fig. 5b). The introduction of ROF decreases the density of scale crystals, causing them to appear more rounded and well-dispersed with a smooth texture (Fig. 5c). In contrast, with the addition of ROFU, a more dispersed and uniform distribution of the crystals is observed as well as decreased crystal density and finely distributed aggregates in smaller clusters implying suppressed crystal nucleation and growth.

From the SEM images in Figs. 4 and 5 for ROF and ROFU, it may suggest that their chemical structures impacted the growth of the scale crystals as their addition to the brine either enhanced/reduced the diameter of $CaCO_3$ and $CaSO_4$ scale crystals as applicable [20-22].

3.5 Performance Evaluation of ROF and ROFU as Scale Inhibitors

The inhibition performance efficiency (IE) of the formulated inhibitors, ROF and ROFU, was evaluated compared to a commercial scale inhibitor (CSI). The data plots in Figs. 6 and 7 reveal the effect of temperature (71°C and 90°C). The data plots in Figs. 6 to 11 contact time (4 and 22 hours at 71°C) and inhibitor concentration (20 to 100 ppm) on the performance of ROF, ROFU, and CSI in inhibiting $CaSO_4$ and $CaCO_3$ scales.
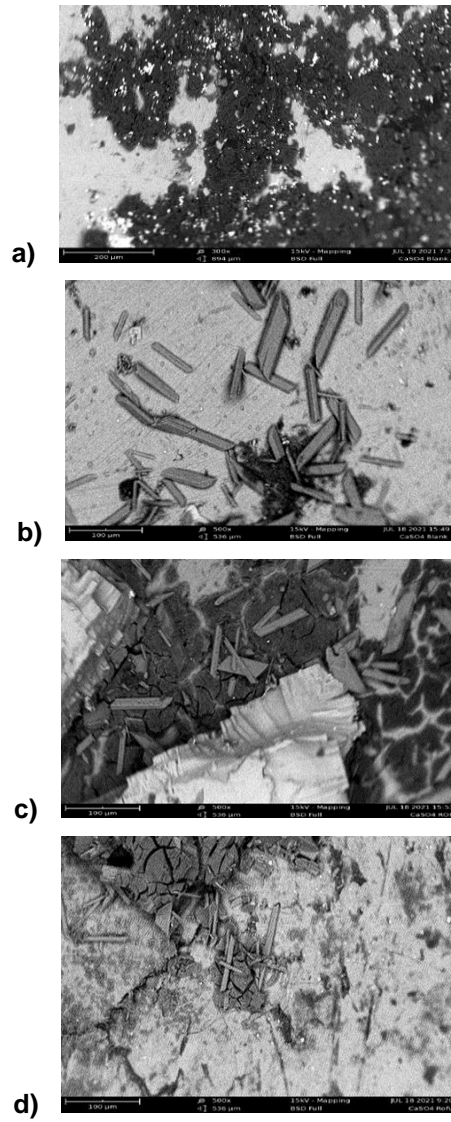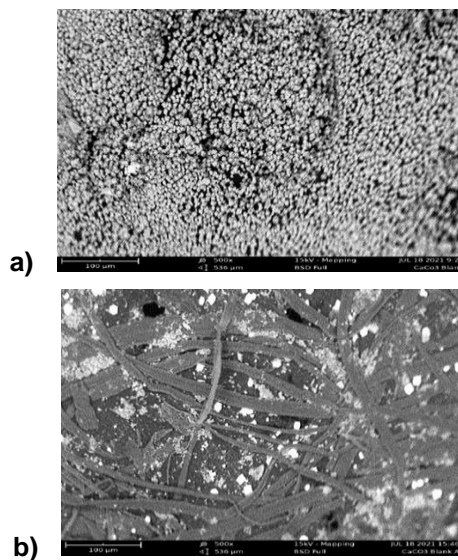
Fig. 4. **SEM micrograph for CaSO₄ scale deposit (a) before conditioning, (b) after conditioning, (c) inhibited with ROF, and (d) inhibited with ROFU**
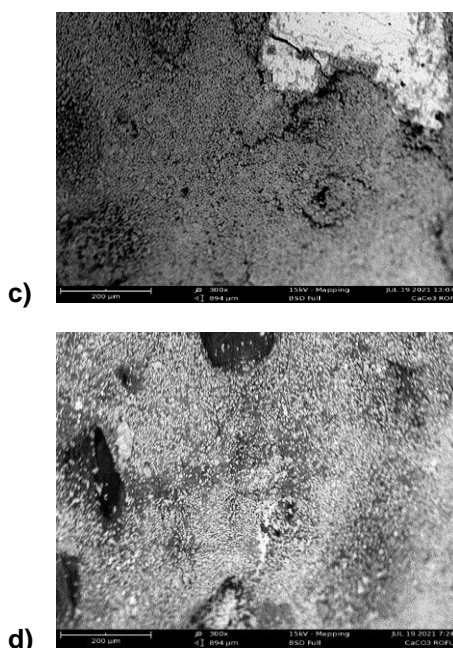
Fig. 5. SEM micrograph for CaCO₃ scale deposit (a) before conditioning, (b) after conditioning (c) inhibited with ROF, and (d) inhibited with ROFU

3.5.1 Temperature effect

Figs. 6 and 7 show comparative plots illustrating the temperature effect of ROF, ROFU, and CSI inhibition performance at 71 °C to 90 °C for CaCO₃ and Fig. 7 for CaSO₄ scales, respectively. For ROF, a slight decrease in CaSO₄ scale inhibition values of 69.15 % and 68.69 % at 100 ppm and 80 ppm was observed at 71 °C and 90 °C, respectively (Fig. 7a). This reflects a negligible drop with an increase in temperature. However, an increase in scale inhibition performance from 52.86 % to 58.82 % at 100 ppm was observed for CaCO₃ scales as the evaluation temperature increased from 71 °C to 90 °C (Fig. 6a). This aligns with studies that indicate elevated temperatures enhance the growth of CaCO₃ scales, thus requiring increased inhibitor concentration for better efficiency [12,23-25].

A similar trend was also observed for ROFU and CSI, as their inhibition performance in CaCO₃ scales increased from 48.92% and 92.50 % (at 71 °C) to 50.73% and 98.36% (at 90 °C) (Fig. 4b and 4c) and also decreased in CaSO₄ scales from 60.38% and 75.26% (at 71 °C) to 55.07% and 68.51% (at 90 °C), respectively at 100 ppm (Fig. 7b and 7c). The evaluated scale inhibitors, ROF, ROFU, and CSI, showed optimal inhibition values in CaSO₄ scales at 71 °C, while in CaCO₃ scales, optimal inhibition values were observed

at 90 °C. Summarily, optimal inhibition rates were observed at higher temperatures of 90 °C than at 71 °C, suggesting that temperature increase influenced the scale inhibitor's performance, causing more inhibitors to be adsorbed onto the scale crystal. Compared to the higher inhibition values of CSI, we can infer that the inhibition performance of ROF and ROFU is above average and favorably inhibited CaSO₄ scales than CaCO₃ scales.

3.5.2 Contact time effect

The study examined the impact of contact time on the inhibition of CaSO₄ and CaCO₃ scales at 4 and 22 hours, as shown in Figs. 8 and 9, respectively. A similar trend was observed across the inhibitors evaluated for the scale types studied: longer contact time (22 hrs) led to increased inhibition performance, suggesting that the length of inhibitor-scale contact plays an integral role in the continuous inhibition of scales, particularly the CaSO₄ and CaCO₃ scales. The scale inhibition values increased steadily, with optimal values recorded in CaSO₄ scales than in CaCO₃ scales except for CSI, which showed higher inhibition values in CaCO₃ than in CaSO₄ scales. As concentration increased, the effect of contact time on CSI's ability to inhibit performance on the CaSO₄ scale showed some variations over time, as shown in Fig. 8c. However, with the studied scales, the difference

61

in inhibition efficiency (IE) is minimal with extended contact times. Overall, the data suggests that for both scale types and inhibitors evaluated, ROF and ROFU, increasing the contact time between the scale and the inhibitor improves its performance [12].
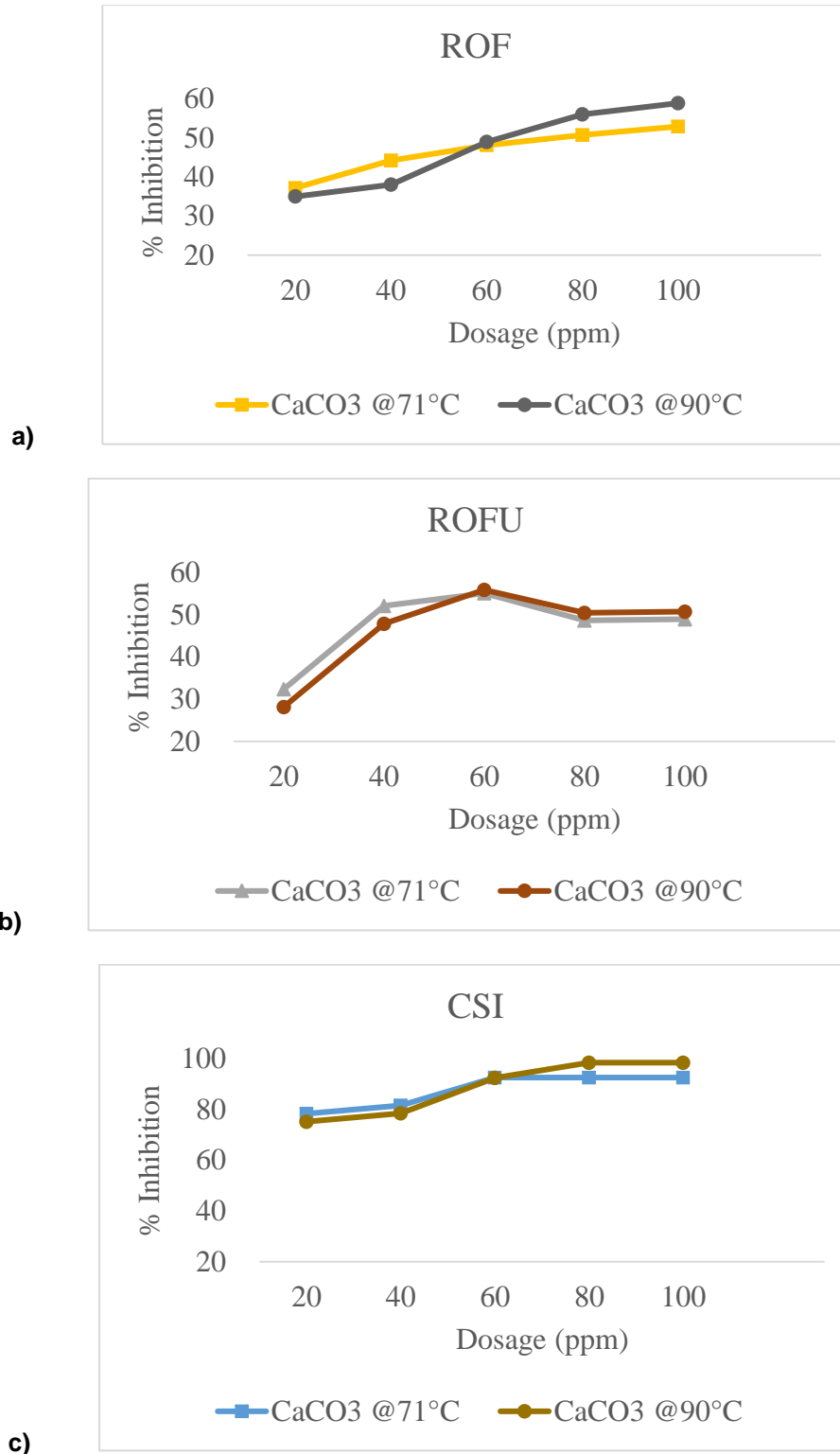

a)

b)

c)

Fig. 6. Effect of temperature on the performance of (a) ROF, (b) ROFU, and (c) CSI on CaCO₃ scales at 71℃ and 90℃ at 22 hrs, respectively
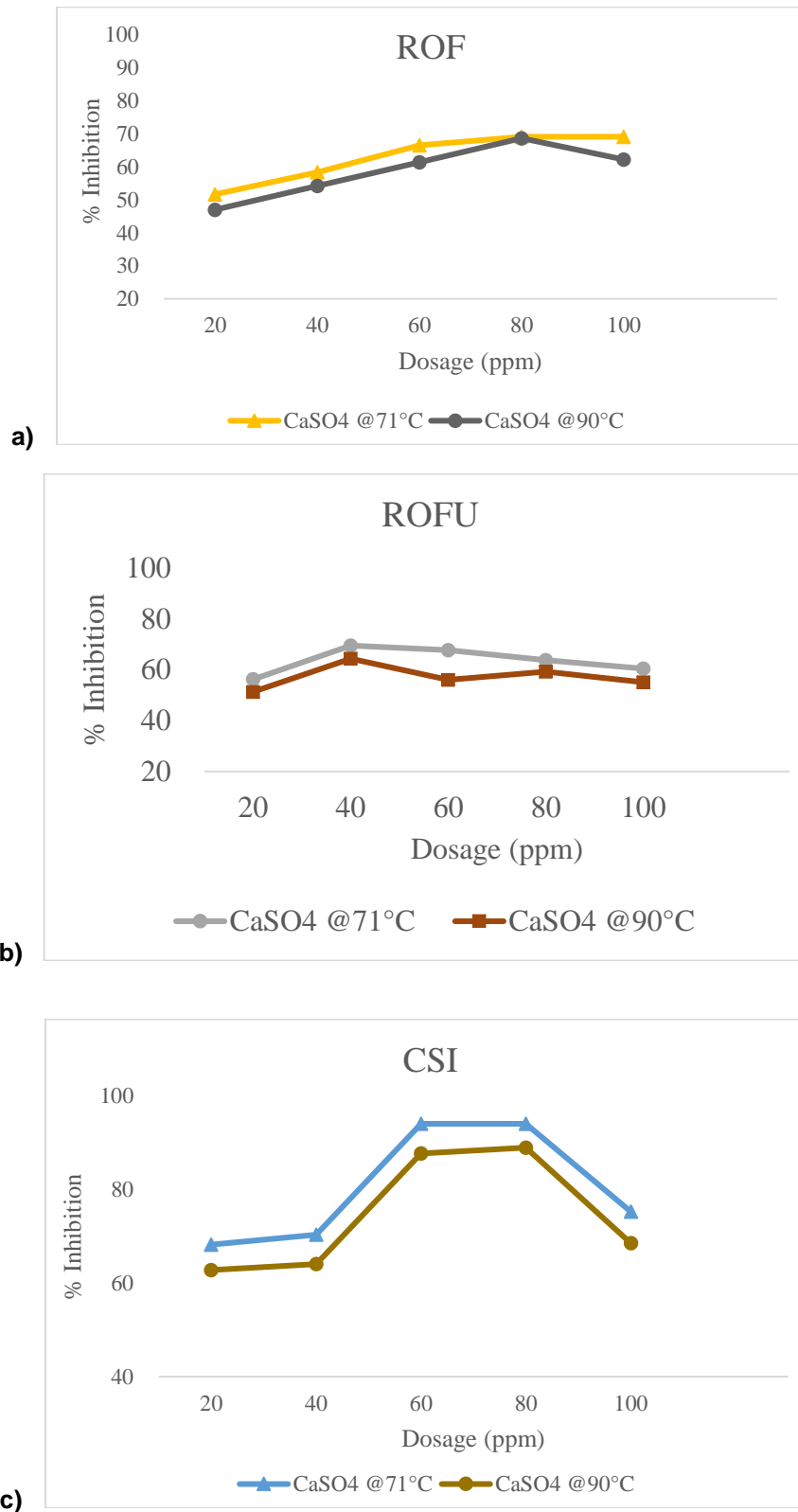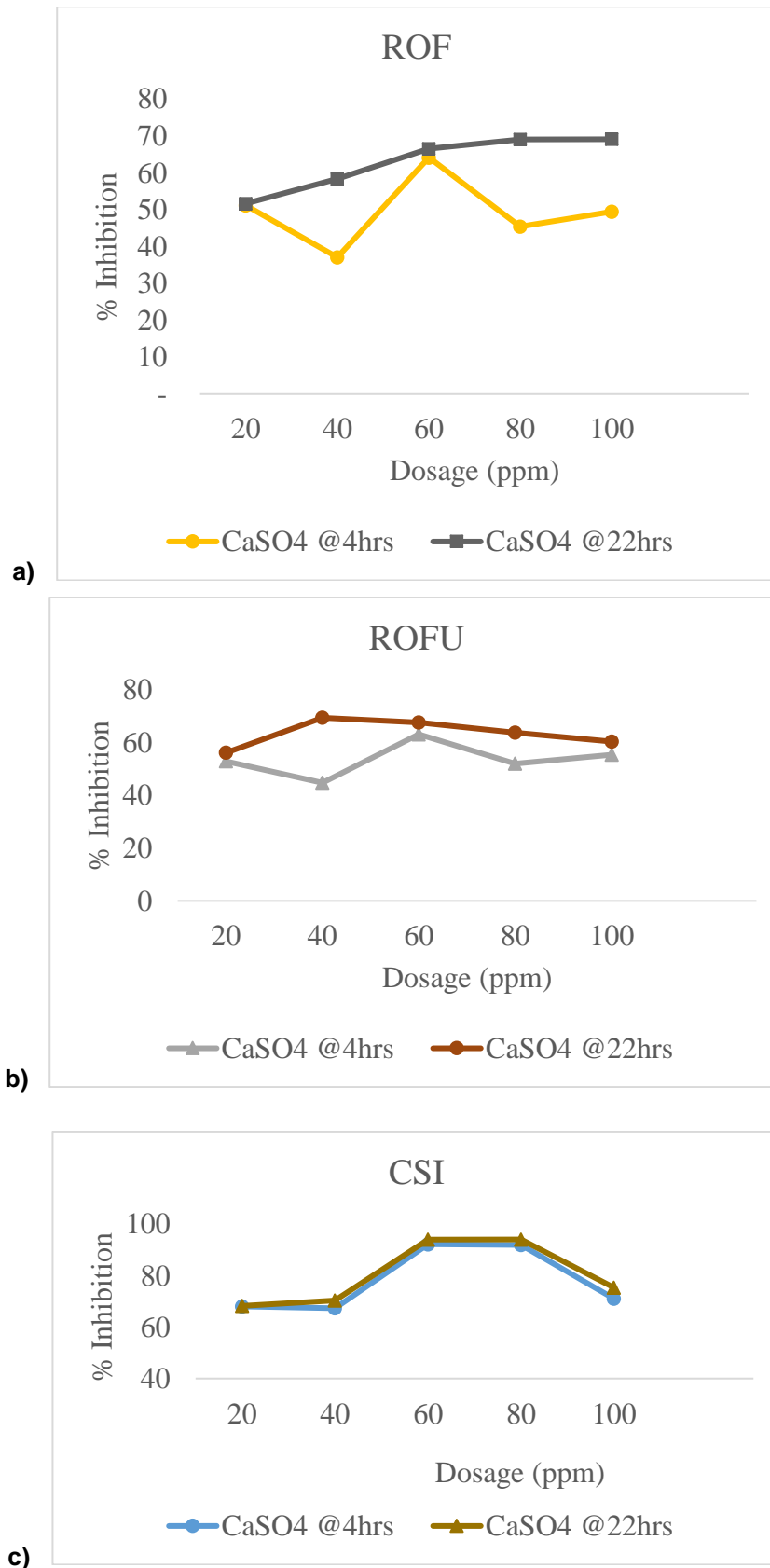
Fig. 7. Effect of temperature on the performance of (a) ROF, (b) ROFU, and (c) CSI on CaSO₄ scales at 71℃ and 90℃ at 22hrs, respectively

Fig. 8. Effect of contact time on the performance of (a) ROF, (b) ROFU, and (c) CSI on CaSO$_4$ scales at 4 hrs and 22 hrs at 71℃ respectively
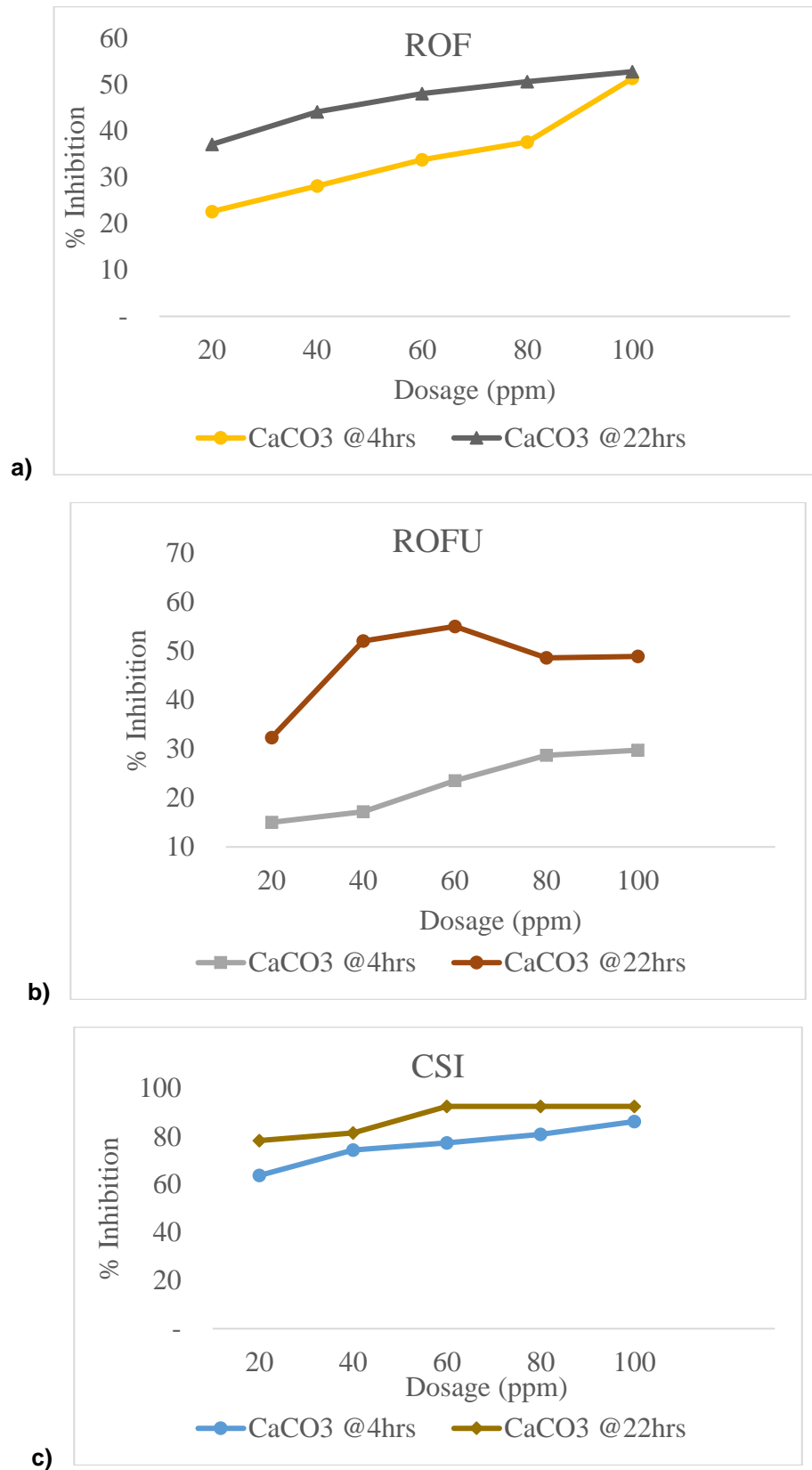
Fig. 9. Effect of contact time on the performance of (a) ROF, (b) ROFU, and (c) CSI on CaCO$_3$ scales at 4 hrs and 22 hrs at 71℃ respectively

3.5.3 Concentration effect

The effect of concentration on scale inhibition using ROF, ROFU, and CSI at different inhibitor dosages (20 ppm to 100 ppm) was evaluated at 71 °C and 90 °C for 22 hours and is shown in Figs. 10 and 11 for $CaSO_4$ and $CaCO_3$ scales, respectively. Generally, increasing the inhibitor dosage for the studied inhibitors increased the inhibition efficiency [12,17,26]. However, once optimum inhibition is achieved, the inhibition rate either remains constant or slowly declines with increasing concentration. A comparative analysis of the formulated SIs with a commercial scale inhibitor, CSI, showed similar inhibition pattern for $CaSO_4$ and $CaCO_3$ scales with over 90% inhibition rate observed with the attainment of optimal inhibition at a minimal dosage of 60 ppm.

Despite the high inhibition rate observed for CSI across the studied scale types, ROF and ROFU show inhibition potential as oilfield green scale inhibitors. ROFU attained optimal inhibition of 69.45% and 55.05 % at 71 °C, 64.30% and 55.85% at 90 °C, and lower concentrations of 40 ppm and 60 ppm, while for ROF, optimal inhibition of 69.15% and 52.86% at 71 °C and 100 ppm, 68.69% and 58.82% at 90 °C, and concentrations of 80 ppm and 100 ppm for $CaSO_4$ and $CaCO_3$ scales for 22 hours, respectively.

3.5.4 Effect of chemical structure

From the inhibition data of the formulated scale inhibitors, we can infer that ROF effectively inhibited $CaCO_3$ scales. At the same time, ROFU
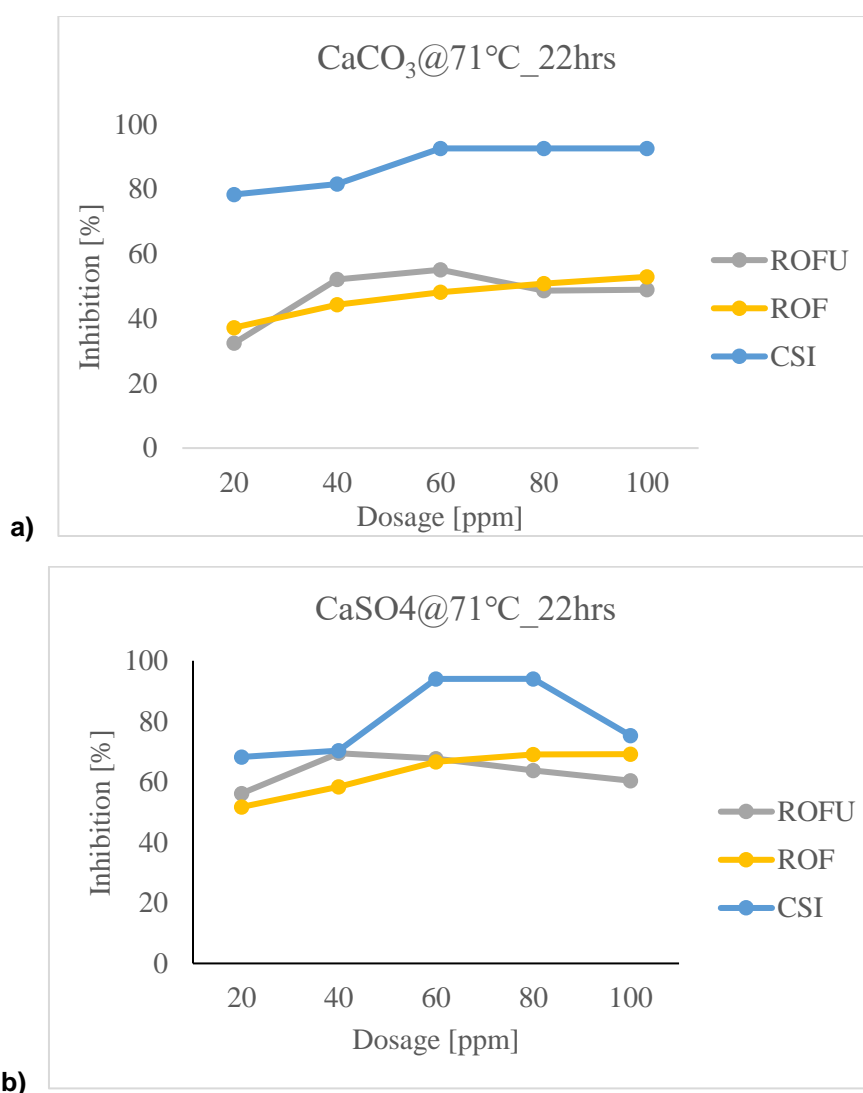

a)

b)

Fig. 10. **Effect of concentration on the inhibitor performance of (a) CaCO$_3$ scales and (b) CaSO$_4$ scales at 22 hrs and 71℃**
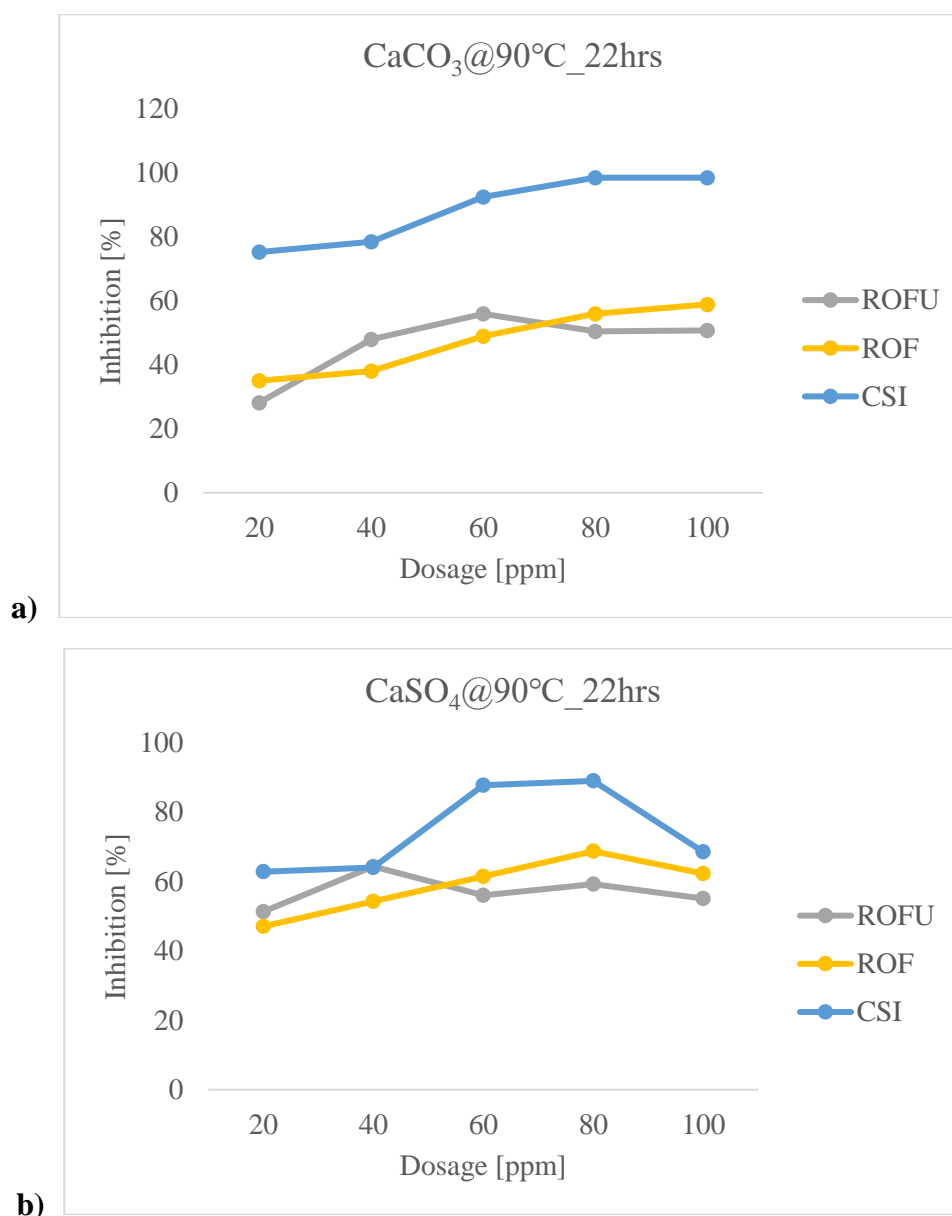
Fig. 11. Effect of concentration on the inhibitor performance of (a) CaCO₃ scales and (b) CaSO₄ scales at 22 hrs and 90℃

showed high inhibition values for CaSO₄ scales, with longer contact times and/or increased temperature and concentration dosage. This may be attributed to the increased number of hydroxyl groups introduced into the ROSE moiety during the chemical modification of ROF with urea via the introduction of amide groups [17,27].

4. CONCLUSION

The scale-inhibiting potential of a potential green oilfield scale inhibitor derivatized via chemical modification of red onion skin extract (ROSE)

with furfuraldehyde (ROF) and urea (ROFU) on Calcium sulfate and carbonate scales has been evaluated. From compatibility and thermal stability studies, the formulated scale inhibitor blends, ROF and ROFU, were found to be thermally stable, highly soluble, and compatible with the simulated brine. Using the NACE standard static bottle test method, the performance evaluations showed that ROF and ROFU are more effective in inhibiting the growth of CaSO₄ scales than CaCO₃ scales, as moderately high IE of 69.15% and 69.45% for CaSO₄ scales, unlike the lower IE values; 51.42% and 29.77% observed for CaCO₃ scales,

at the studied concentration range. From the inhibition data, we can infer that ROF effectively inhibited $CaCO_3$ scales. At the same time, ROFU showed high inhibition values for $CaSO_4$ scales, with longer contact times and/or increased temperature and concentration dosage. This may be attributed to the increased number of hydroxyl groups introduced into the ROSE moiety during the chemical modification of ROF with urea via the introduction of amide groups. Unlike other studies, it was observed that temperature increase had a negligible impact on the inhibition rate for all the inhibitors and both scale types. However, their IE increased with the contact time, as the formulated inhibitors both demonstrated continuous scale inhibition action. Contrary to the $CaSO_4$ scale, which requires lower temperatures, the $CaCO_3$ scale requires high temperatures and inhibitor concentrations for effective inhibition. Based on literature findings, increasing inhibitor concentration is required for improved efficiency since higher temperatures promote the development of $CaSO_4$ scales [12,17,23,24,26]. In conclusion, the performance of the formulated SIs, though slightly lower across the concentration range studied for $CaCO_3$ and $CaSO_4$ scales, compared favorably with CSI in terms of their ability to inhibit and, as a result, reveal they can be considered potentially inexpensive, renewable, eco-friendly, and effective green oilfield scale inhibitor alternatives for $CaSO_4$ scales. Furthermore, modification on the composition of these bio-resins and investigation of their adsorption mechanism are recommended for further studies. The information given will further enable research into the application of ROSE derivatives as green oil field scale inhibitors.

DISCLAIMER (ARTIFICIAL INTELLIGENCE)

Author(s) hereby declare that NO generative AI technologies such as Large Language Models (ChatGPT, COPILOT, etc) and text-to-image generators have been used during writing or editing of this manuscript.

FUNDING

AVAILABILITY OF DATA AND MATERIALS

All the datasets generated during this study are available on reasonable request.

ACKNOWLEDGMENTS

COMPETING INTERESTS

Authors have declared that no competing interests exist.

REFERENCES

1. Hatti-Kaul R, Törnvall U, Gustafsson L, Börjesson P. Industrial biotechnology for the production of bio-based chemicals–a cradle-to-grave perspective. Trends in biotechnology. 2007;25(3):119-124.

2. Ituen EB, Ime-Sunday JI, Essien EA. Inhibition of oilfield scales using plant materials: A peep into green future. Chemistry Research Journal. 2017;2(5): 284-292.

3. Verma C, Chauhan DS, Aslam R, Banerjee P, Aslam J, Quadri TW, Zehra S, Verma DK, Quraishi MA, Dubey S, AlFantazi A, Rasheed T. Principles and theories of green chemistry for corrosion science and engineering: design and application. Green Chemistry. 2024;26(8): 4270-4357.

4. Benyus JM. Biobased Materials. Materials Matter: Toward a Sustainable Materials Policy. 2001;283-304.

5. Powell RW, Elton C, Prestidge R, Belanger H. Biobased chemicals and polymers. Plant biomass conversion. 2011;275-309.

6. Jessop PG, Ahmadpour F, Buczynski MA, Burns TJ, Green Ii NB, Korwin R, Long D, Massad SK, Manley JB, Omidbakhsh N, Pearl R, Wolf MH. Opportunities for greener alternatives in chemical formulations. Green Chemistry. 2015;17(5): 2664-2678.

7. Jessop PG, Reyes LM, Kelley SP, Berton P, Metlen A, Rogers RD, Gutowski KE, Sliva PG, Neff R, Gajewski A, Kuo PY, Lingwood MD. Green Chemistry in Industry. Walter de Gruyter GmbH & Co KG. 2018;3.

8. Li S, Qu Q, Li L, Xia K, Li Y, Zhu T. Bacillus cereus s-EPS as a dual bio-functional corrosion and scale inhibitor in artificial seawater. Water Research. 2019; 166:115094.

9. Abdel-Raouf ME, Keshawy M, Hasan AM. Green polymers and their uses in petroleum industry, current state and future perspectives. Crude Oil-New Technologies and Recent Approaches; 2021.

10. Verma D, Fortunati E. Biopolymer processing and its composites: An introduction. In Biomass, biopolymer-based materials, and bioenergy. Woodhead Publishing. 2019;3-23.

11. Dickinson W, Sanders L, Lowen C. Development and performance of biodegradable antiscalants for oilfield applications. In Offshore Technology Conference. OTC. 2011; OTC-21788.

12. Victor-Oji CO, Una D, Joseph A, Appah D, Akaranta O. Performance evaluation of glutaraldehyde-modified red onion skin extract as oilfield scale inhibitors. Petroleum Science and Technology. 2024;1-22.

13. Obuebite AA, Victor-Oji CO, Eke WI. Laboratory evaluation of red onion skin extract and its derivative as biomass-based enhanced oil recovery agents. Scientific African. 2023a ;19: e01460.

14. Obuebite AA, Eke WI, Victor-Oji C, Una DC, Akaranta O. Comparative performance evaluation of modified red onion skin extract as surface active agents for tertiary oil recovery. Energy Sources, Part A: Recovery, Utilization, and Environmental Effects. 2023b;45(2):5096-5109.

15. Phung Hai TA, Tessman M, Neelakantan N, Samoylov AA, Ito Y, Rajput BS, Pourahmady N, Burkart MD. Renewable polyurethanes from sustainable biological precursors. Biomacromolecules. 2021; 22(5):1770-1794.

16. Tenorio-Alfonso A, Sánchez MC, Franco JM. A review of the sustainable approaches in the production of bio-based polyurethanes and their applications in the adhesive field. Journal of Polymers and the Environment. 2020;28: 749-774.

17. Una D, Appah D, Amieibibama J, Eke WI, Akaranta O. Structure-property relationship of flavonoids as potential green inhibitors for oilfield scales: A mini-review. Journal of Engineering Research and Reports. 2021;21(6):41-51.

18. Mavredaki E, Neville A, Sorbie KS. Initial stages of barium sulfate formation at surfaces in the presence of inhibitors. Cryst Growth Des. 2011;11:4751–4758.

19. Shen D, Shcolnik D, Perkins R, Taylor G, Brown M. Evaluation of scale inhibitors in Marcellus high-iron waters. Oil and Gas Facilities. 2012;1(05):34-42.

20. El-Said M, Ramzi M, Abdel-Moghny T. Analysis of oilfield waters by ion chromatography to determine the composition of scale deposition. Desalination. 2009;249(2):748-756.

21. Ohimor OE, Anigboro OE, Anih CE, Ononiwu PI. Performance evaluation of biodegradable oilfield scale inhibitors for calcium carbonate scales. International Journal of Emerging Trends in Engineering and Development. 2019;3(9): 34-46.

22. Hoang TA. Mechanisms of scale formation and inhibition. In Water-formed deposits. Elsevier. 2022; 13-47.

23. Dyer SJ, Graham GM. The effect of temperature and pressure on oilfield scale formation. Journal of Petroleum Science and Engineering. 2002;35(1-2):95-107.

24. Olajire AA. A review of oilfield scale management technology for oil and gas production. Journal of petroleum science and engineering. 2015;135:723-737.

25. Zhao Y, Xu Z, Wang B, He J. Scale inhibition performance of sodium carboxymethyl cellulose on heat transfer surface at various temperatures: Experiments and molecular dynamics simulation. International Journal of Heat and Mass Transfer. 2019;141:457-463.

26. Spinthaki A, Kamaratou M, Skordalou G, Petratos G, Petrou I, Tramaux A, David G, Demadis KD. Searching for a universal

scale inhibitor: A multi-scale approach towards inhibitor efficiency. Geothermics. 2021;89:101954.

27. NACE International. NACE Standard TM0197: Laboratory screening test to determine the ability of scale inhibitors to prevent the precipitation of barium sulfate or strontium sulfate, or both, from solution (for Oil AND Gas Production Systems); 2010.

Peer-review history:
The peer review history for this paper can be accessed here:
https://www.sdiarticle5.com/review-history/123518